Supported Membranes with Well-Defined Polymer Tethers—Incorporation of Cell Receptors

Oliver Purrucker,[a] Anton Förtig,[b] Rainer Jordan,*[b, c] and Motomu Tanaka*[a]

*We report the design of supported lipid membranes attached to the surface by tailored lipopolymer tethers. A series of well-defined lipopolymers were synthesized by means of living cationic polymerization of 2-methyl-2-oxazolines. The polymers were equipped with a silane coupling group on the proximal, and lipid anchors on the distal chain ends. The length of the intermediate hydrophilic polymer tether was varied (*n = *14, 18, 33) to change the distance between the membrane and the substrate. Supported membranes have been prepared in two-steps. First, a suitable lipopolymer/lipid mixture was deposited by Langmuir–Blodgett transfer, and annealed to establish the covalent coupling to the surface. On the dry lipopolymer/lipid monolayer, the upper leaflet was deposited by vesicle fusion. Optimization of both preparation steps resulted in the formation of stable and defect-free membranes. Impacts of the spacer length and the lipopolymer fraction upon the lateral diffusivity of the lipids were systematically compared by fluorescence recovery after photobleaching (FRAP). First experiments on the incorporation of a large transmembrane cell receptor (integrin $\alpha_{IIb}\beta_3$) into the polymer-tethered membrane suggested that the length of the polymer tether plays a crucial role in distribution of the proteins on the surface.*

Introduction

Supported lipid membranes have been intensively and widely investigated in the last decades as a general model of plasma membranes.[1–3] Especially, a supported membrane with cell surface receptors such as integrin, cadherin, or intercellular adhesion molecules can provide an artificial model to mimic cellular surfaces to study physical principles of cell–cell and cell–tissue interactions.[4–8]

A conventional method is to incorporate transmembrane proteins into lipid vesicles (proteoliposomes) from surfactant micelles, and spread them on hydrophilic solid substrates. However, in spite of several previous reports, it is still difficult to reconstitute proteins orientation-selectively and furthermore; the close proximity of the artificial membrane to the solid support with a typical distance of 5–20 Å[9–12] does not provide a sufficient water reservoir that even causes nonspecific adsorption and denaturing of proteins. Especially, the latter is a serious problem for most of the cell adhesion proteins that have intracellular domains larger than 10 nm. This problem can be overcome by introduction of hydrophilic polymer interlayers, such as polymer "cushions"[13] and polymer "tethers",[14] which can provide more "fluid" environments for proteins.

As polymer "cushions", we demonstrated that Langmuir–Blodgett (LB) films of regenerated cellulose (thickness: 5 to 10 nm) could serve as a good template for deposition of model and native cell membranes. For example, an artificial lipid bilayer deposited onto indium–tin oxide (ITO) electrodes coated with a cellulose LB film had an electric resistance of 0.5 MΩ cm^2,[15] which was by a factor of five larger than that obtained for the membranes deposited directly onto ITO.[16] Furthermore, it has been demonstrated that human erythrocyte membranes can homogeneously be deposited on cellulose LB films, where their native orientation was selectively maintained on the surface.[17] More recently, Gönnenwein et al. have spread proteoliposomes with integrin $\alpha_{IIb}\beta_3$ on cellulose films and measured the lateral diffusion constant and the adhesion strength against the selective ligands. The mobility and functionality of the immobilized integrins in polymer-supported membranes were found to be larger than those in the glass-supported membranes.[8]

An alternative strategy to decouple a lipid bilayer from a solid support without loosing the stability is the incorporation of lipopolymer tethers.[14, 18, 19] Such tethers are equipped with surface-coupling groups for attachment to the solid surface, lipid anchors for insertion into the membrane, and a connecting hydrophilic and flexible polymer chain that keeps a certain distance between the substrate and the membrane. One of the possible macromolecular architectures is a random terpolymer of functional monomers,[20–23] where the final morphology

[a] *O. Purrucker, Dr. M. Tanaka*
Lehrstuhl für Biophysik, Technische Universität München
James-Franck-Strasse, 85748 Garching (Germany)
Fax: (+49) 89-289-12469
E-mail: mtanaka@ph.tum.de

[b] *A. Förtig, Dr. R. Jordan*
Lehrstuhl für Makromolekulare Stoffe, Technische Universität München
Lichtenbergstr. 4, 85748 Garching (Germany)
Fax: (+49) 89-289-13562
E-mail: rainer.jordan@ch.tum.de

[c] *Dr. R. Jordan*
Department of Chemistry, Chemical Engineering and Materials Science
Polytechnic University, Six Metrotech Center
Brooklyn NY 11201 (USA)

 DOI: 10.1002/cphc.200300863

depends on the ratio between three monomers. However, it was still difficult to control the phase separation between hydrophobic and hydrophilic layers due to the random distribution of each building block, which often resulted in local defects. Another possibility is to incorporate lipopolymers with defined polymer spacers.[18] This defined macromolecular architecture was realized for functional polymers based on oligo-[24–27] and poly(ethylenoxide),[28, 29] and oligopeptides with thiol groups.[30, 31] Lipopolymers with poly(2-oxazoline) spacers[32–36] have certain advantages, since the living cationic polymerization allows for flexible synthesis of tailored lipopolymers with different surface coupling groups, length and side functionalities of the spacers.

Fabrication of homogeneous and stable membranes demands quantitative control of length and lateral density of the polymer spacers, as well as the clear separation between hydrophilic polymer chains and hydrophobic membrane anchors. The first point is important to control the thickness and viscosity of the water reservoir between the substrate and the membrane, while the second, selective hydration of the polymer spacer, is crucial to avoid formation of local defects due to the negative spreading pressure.[37, 38] Our previous study demonstrated that linear connection of lipid anchors and polymer spacers improved the separation of two components for grafted lipopolymer films.[32] We observed the formation of a layered morphology of 2-oxazoline lipopolymers grafted on surfaces, simply induced by selective swelling with water. The resulting layer structure was found to correlate with the polymer composition.[32] However, the mismatch of the cross sectional area of the lipid anchors and polymer tethers is not suitable for a direct preparation of a lipid bilayer by self-assembly.

In 2000, Wagner and Tamm reported the deposition of supported membranes with silane-functionalized poly(ethylenoxide) tethers ($n = 77$) on glass substrates.[28] A mixed monolayer of lipids and lipopolymers was transferred onto a substrate by Langmuir – Blodgett (LB) deposition, followed by the fusion of vesicle suspensions to form the upper leaflet of a lipid bilayer. Naumann et al. took a similar strategy, using a poly(2-ethyl-2-oxazoline) lipopolymer ($n = 85$) for tethering lipid membranes.[36] Instead of the surface-reactive group at the end of the polymer chain, the lipid/lipopolymer monolayer was randomly grafted onto the surface by a photocrosslinking reaction using grafted benzophenone derivatives. These two systems have been tested for the incorporation of several transmembrane proteins (cytochrome b5, annexin V, ATPase, etc.), but the systematic control of the length and density of the polymer tethers is still missing.

In this study, we designed a new type of polymer-tethered membrane with defined ($n = 14$, 18, and 33) poly(2-methyl-2-oxazoline) chains. Each lipopolymer studied here consists of dioctadecyl lipid anchors, a glycerol junction, a hydrophilic poly(2-methyl-2-oxazoline) spacer, and a trifunctional silane-coupling group. Recently, we reported quantitative measurements of hydration properties of poly(2-oxazoline) homopolymers with the same silane functional groups (i.e., spacers without lipid anchors) using ellipsometry, confirming a good water storage capability of poly(2-oxazoline) layers.[39] As schematically illustrated in Figure 1, the polymer-tethered membrane was prepared according to the protocol reported by Wagner and Tamm.[28] Each step of the preparation was carefully optimized, and the homogeneity and fluidity of the membrane were checked as a function of molar fraction (density) and length of the polymer spacers, using fluorescence microscopy and fluorescence recovery after photobleaching (FRAP) technique. As a preliminary challenge to incorporate transmembrane cell receptors, proteoliposomes with integrin $\alpha_{IIb}\beta_3$ were spread on the monolayers with various spacers. Details of the obtained results will be described in the following sections.

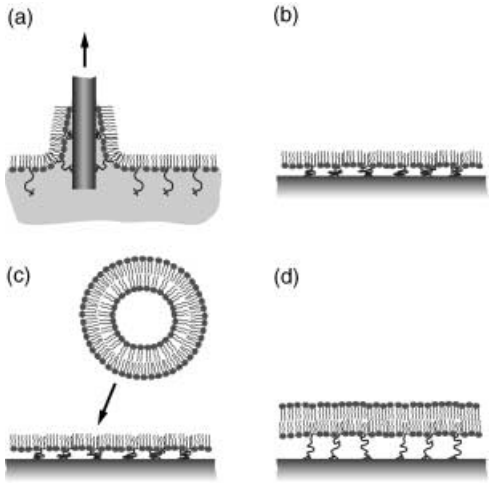

Figure 1. *Schematic illustration of the stepwise preparation of a polymer-tethered membrane: a) Langmuir – Blodgett (LB) transfer of a lipid/lipopolymer monolayer, b) grafting of lipopolymers by annealing, and c,d) spreading of the upper monolayer by vesicle fusion.*

Materials and Methods

Materials

1-Stearoyl-2-oleoyl-*sn*-glycero-3-phosphocholine (SOPC) and 1-oleoyl-2-[12-[(7-nitro-2 – 1,3-benzoxadiazol-4-yl)amino]dodecanoyl]-*sn*-glycero-3-phosphocholine (NBD-PC) were purchased from Avanti Polar Lipids (Alabaster, USA), 1,2-dihexadecanoyl-*sn*-glycero-3-phosphoethanolamine triethylammonium salt (Texas Red-PE) was from Molecular Probes (Leiden, Netherlands). Freshly distilled and deionized water (Millipore, France, $R >$ 18 MΩ cm) was used for the preparation of buffer solutions containing 10 mM 4-(2-hydroxyethyl)piperazine-1-ethanesulfonic-acid (Hepes, pH 7.5) and additional 50 mM NaCl, which were degassed before each measurement.

1,2-*O*-Dioctadecyl-*sn*-glycero-3-trifluormethanesulfonate was prepared from 1,2-*O*-dioctadecyl-*sn*-glycerol (BACHEM, Weil am Rhein, Germany) and trifluoromethanesulfonic anhydride (Fluka, Neu-Ulm, Germany). The 2-methyl-2-oxazoline (Sigma-Aldrich, München, Germany) was stirred over CaH_2 (Sigma-Aldrich) and as well as 3-aminopropyltrimethoxysilane (ABCR, Karlsruhe, Germany) freshly distilled prior to use.

For the preparation of integrin containing lipid vesicles, the following materials were used:

Triton X-100 was purchased from Aldrich, Bio-Beads SM2 adsorbents from Bio-Rad Laboratories (Hercules, USA), 1,2-dimyristoyl-*sn*-glycero-3-phosphocholine (DMPC) and 1,2-dimyristoyl-*sn*-glycero-3-[phospho-*rac*-(1-glycerol)] (DMPG) from Avanti Polar Lipids. Integrins were labeled with 5-(and-6)-carboxytetramethylrhodamine, succinimidyl ester (5(6)-TAMRA-SE), purchased from Molecular Probes. Buffer solutions were prepared with tris-(hydroxymethyl)-aminomethane (Tris), purchased from Roth GmbH (Karlsruhe, Germany).

Glass cover slides (24 × 24 mm) from Karl Hecht KG (Sondheim, Germany) were used as solid supports. Prior to the film deposition, they were cleaned in the following manner: After rinsing with acetone and methanol, the samples were immersed into a solution of 1:1:5 (v/v) H_2O_2 (30%):NH_4OH (30%):H_2O for 5 min under ultrasonication, and soaked for another 30 min at 60 °C.[40] Finally, they were rinsed intensively with water, dried at 70 °C and stored in sealed glass boxes. All other chemicals were purchased from Sigma-Aldrich and used without further purification.

Synthesis of Silane-Functionalized Lipopolymers

The polymerization and purification were carried out under a dry nitrogen atmosphere using the Schlenk technique. All solvents were freshly dried and distilled prior to use. The detailed preparations, such as purification of solvents and monomers, synthesis of the lipid initiator, polymerization and purification of the polymer, were carried out analog to our previously published account.[33, 34] Only here, 2-methyl-2-oxazoline was used as the monomer and 3-aminopropyltrimethoxysilane as the terminating agent. The resulting lipopolymer was kept under anhydrous conditions to avoid hydrolysis and polycondensation of the trimethoxysilane groups. Typical polymerization procedure (POX14, $n = 14$) in short:

423 mg (4.9 mmol) of freshly distilled 2-methyl-2-oxazoline was added to a solution of 354 mg (0.49 mmol) 1,2-*O*-dioctadecyl-*sn*-glycero-3-trifluoromethanesulfonate[33] in 40 mL $CHCl_3$ at 0 °C. The cold vessel was sealed and transferred to a preheated oil bath (60 °C) and refluxed for 30 h. For functionalization via the termination reaction, the reaction mixture was cooled again to 0 °C and 1.227 g (6.8 mmol) of freshly distilled 3-aminopropyltrimethoxysilane was added. The mixture was stirred at room temperature over night. After removal of most of the solvent, the polymer was precipitated in 300 mL of dry diethyl ether at 0 °C. After filtration (PTFE filter $\Phi = 0.45$ μm; Sartorius, Göttingen, Germany), the polymer was dissolved in 10 mL $CHCl_3$ and stirred with 1 g of potassium carbonate over night. The mixture was filtered, reprecipitated ($CHCl_3$/diethyl ether) and freeze-dried using dry benzene, to give 0.497 g (yield: 63%) of a colorless powder.

For the synthesis of longer lipopolymers (POX18, POX33; with $n = 18$, 33) the corresponding initiator-to-monomer ratio and longer reaction times were used. All polymers were characterized by ^{1}H NMR spectrometry and gel permeation chromatography. ^{1}H NMR (300 MHz) spectra were recorded in $CDCl_3$ using an ARX 300 (Bruker, Karlsruhe, Germany). Gel permeation chromatography (GPC) was carried out on a GPC 510 (Waters), using $CHCl_3$ and polystyrene standard for calibration. As reported previously, the end-functionalization was confirmed to be quantitative (Table 1). The differences in the polymer analytical values are common when different techniques are used. For a detailed discussion and analysis of the reliability of these characterization techniques for amphiphilic and functionalized poly(2-oxazoline)s please refer to our previous accounts.[41]

Table 1. *Characterization of used lipopolymers.*

Lipopolymer	$[M]_0/[I]_0$[a]	t [h][b]	NMR DP_n[c]	GPC PDI[d]	Yield [%][e]
POX14	10	30	14	1.09	63
POX18	20	40	18	1.33	86
POX33	40	50	33	1.30	75

[a] Initial monomer/initiator feed. [b] Polymerization time. [c] Degree of polymerization calculated from the ^{1}H NMR spectra (end group analysis). [d] Polydispersity index ($\bar{M}_w/\bar{M}_n$). [e] Yield calculated versus initial initiator amount.

^{1}H NMR (300 Mhz, $CDCl_3$): $\delta = 0.6$ (b, CH_2-Si(OMe)$_3$, 2H); δ 0.86 (t, CH_3-CH_2-, 6H); δ 1.1 – 1.4 (b, $(CH_2)_n$); δ 2.0 – 2.2 (b, CH_3-CO-N); δ 3.3 – 3.6 ppm (b, CH_2-N-CH_2).

Langmuir – Blodgett Deposition of Lipid/Lipopolymer Monolayers

Before spreading of the monolayer onto the air – water interface of a self-built Langmuir trough (subphase area: 982 cm^2), the cleaned, hydrophilic substrates were immersed into the subphase. An appropriate mixture of lipid and lipopolymer (dissolved in chloroform) was spread onto the water subphase. After evaporation of the solvent, the monolayer was compressed to a lateral pressure of 30 mN m^{-1} (barrier speed: 50 μm s^{-1}) at 20 °C, followed by the successive deposition of the monolayer onto the cleaned substrate at a transfer velocity of 400 μm s^{-1}. During the LB transfer, the surface pressure was maintained constant with an electronic feedback circuit. The transfer ratio of 1:1 verified the successful transfer of the monolayer. For fluorescence studies of the dry LB monolayer, 0.2 mol% Texas Red-PE was added to the lipid/lipopolymer mixture before spreading.

Spreading of Top Layers by Vesicle Fusion

For the preparation of polymer-tethered lipid bilayers, lipid vesicle suspensions were directly deposited onto the dry, hydrophobic LB monolayers.[42, 43] These suspensions in a buffer solution were prepared according to the conventional procedures described elsewhere.[15, 44] In short: Appropriate amounts of lipids from a chloroform stock solution were mixed in a glass flask. After evaporation of the solvent, a buffer solution was added to obtain the total lipid concentration of about 1 mg mL^{-1}. The lipid suspension was sonicated for 10 min to create small unilamellar vesicles (SUVs) which were centrifuged at 2500 min^{-1} for 5 min to remove any titanium debits from the

sonicator tip. The vesicle suspensions were deposited onto the LB monolayer, and incubated for several hours at room temperature. The remaining vesicles were removed by intensive rinsing with the buffer solution.

Fluorescence Microscopy

For fluorescence studies, an inverted microscope (Axiovert 200), equipped with a 63x long distance objective (numerical aperture 0.75) and standard fluorescence filter sets, was used (Carl Zeiss, Göttingen, Germany). Images and movies were taken by a cooled CCD camera (Orca ER, Hamamatsu Photonics, Herrsching, Germany), digitized by a frame-grabber card (Stemmer Imaging, Puchheim, Germany), and processed by a home-made imaging software.[45]

Lateral Diffusion of Lipids

To measure the lateral diffusion constant of lipids in the membrane, the under leaflet (underlayer) and the upper leaflet (top layer) of the membrane were selectively labeled with fluorescence lipids. For instance, the underlayer was labeled by doping 1 mol% NBD-PC in the LB monolayer, followed by spreading of unlabeled SOPC vesicles, whereas SOPC vesicles with 1 mol% NBD-PC were spread on the unlabeled monolayers to label the top layer.

Lateral diffusion constant and mobile fraction of lipids in the polymer-tethered membrane were measured by the fluorescence recovery after photobleaching (FRAP) technique.[46] The beam of an argon ion laser (Innova 70, Coherent, Santa Clara, CA, USA) was divided into the bleaching and observation beams (1000-times attenuated), and focused onto the sample (spot diameter 9.3 μm) through a microscope oil immersion objective (Fluar 100x, numerical aperture 1.3, Carl Zeiss, Göttingen, Germany). The dye molecules were bleached by a short laser pulse (200 ms), and recovery of the fluorescence intensity according to the diffusion of unbleached dyes was monitored by a photomultiplier (Hamamatsu Photonics). The lateral diffusion constant D and mobile fraction were calculated from the measured fluorescence recovery profiles, following the method reported by Soumpasis.[47]

Incorporation of Integrin $\alpha_{IIb}\beta_3$

Incorporation of transmembrane proteins was carried out by spreading proteoliposomes onto the dry LB monolayer, following the protocols reported previously:[6, 48, 49] Integrin $\alpha_{IIb}\beta_3$ was extracted from outdated human blood platelets of the local blood bank using Triton X-100,[50] whose specific function was checked by enzyme-linked immunosorbent assay (ELISA) tests. For reconstitution of integrins into lipid vesicles, Triton X-100 was removed by Bio-Beads SM2, as described previously.[6, 48, 49] As matrix lipids, a 1:1 mixture (mol%) of DMPC and DMPG was used. The integrin containing vesicles were dialyzed to 20 mM Tris, 150 mM NaCl, 1 mM $CaCl_2$, 1 mM $MgCl_2$, 1 mM NaN_3 (pH 7.4). For fluorescence microscopy and FRAP experiments, integrins were labeled with 5(6)-TAMRA-SE, whose labeling efficiency was quantified to be 100%.[49] The labeled and unlabeled proteins were mixed to yield a final molar fraction of labeled proteins of 10%. The proteoliposomes were spread onto dry LB monolayers, and incubated for two hours at 40 °C. The supernatant solution was removed by intensive rinsing with buffer solution, containing 10 mM Hepes, 100 mM NaCl, 1 mM $CaCl_2$, 1 mM $MgCl_2$, 1 mM NaN_3 (pH 7.4).

Results and Discussion

Lipopolymer Synthesis

In this study, we prepared a row of 2-methyl-2-oxazoline lipopolymers with a variation of the hydrophilic chain length of $n = 14$, 18, and 33, equipped with a 1,2-*O*-dioctadecyl-*sn*-glyceryl anchor and a trifunctional methoxysilane coupling end group. The synthesis is outlined in Figure 2.

The double chain lipid moiety with ether instead of ester linkages is stable against hydrolysis—analog to lipids found in archaea.[51] In fact, the importance of the ether linkage for preparation of stable membranes was recently postulated by several groups.[27, 52] In contrast to our earlier accounts, 2-methyl-2-oxazoline instead of 2-ethyl-2-oxazoline was used as the monomer. Both monomers resulted in hydrophilic polymers with similar swelling behavior,[39] suppressing unspecific adsorption to proteins.[53–56] However, recent studies revealed adsorption of poly(2-ethyl-2-oxazoline) to the air–water interface, which might result in poorer separation between lipid anchors and polymer spacers.[57–59] In this study, we used trimethoxysilane groups instead of dimethylmethoxysilane groups for surface coupling. Although dimethylmethoxysilane and trimethoxysilane are both suitable coupling groups to SiO_2 surfaces, trifunctional silanes guarantee more effective coupling reaction and higher stability towards hydrolysis. Since the lipopolymers were deposited at relatively low grafting densities, a polycondensation of the silane end groups during or after the LB transfer is negligible.

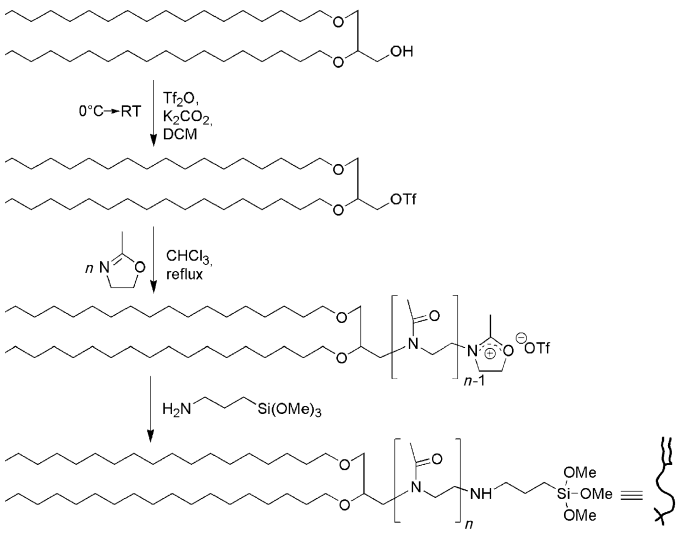

Figure 2. *Reaction scheme for the preparation of silane-functionalized poly(2-methyl-2-oxazoline)s lipopolymers [*n *= 14 (POX14), 18 (POX18), and 33 (POX33)].*

Langmuir Isotherms of Lipid/Lipopolymer Monolayers

As the first step, Langmuir isotherms of various lipid/lipopolymer (POX14) mixtures were measured to determine the optimal mixing ratios (Figure 3a). With increasing molar fractions of lipopolymer, we observed an increase in average area per molecule, corresponding to the larger hydrophilic moiety of the lipopolymers in comparison to that of matrix lipids. At lipopolymer concentrations above 20 mol%, a shoulder-like region appeared, caused by polymer–polymer interactions at surface pressures of $\pi \geq 20$ mN m^{-1}. Although there is a distinct hydrophobic mismatch between lipid anchors of matrix lipid (stearoyl-oleoyl chains) and those of lipopolymer (distearoyl chains), no phase separation could be observed by fluorescence microscopy at the air–water interface.

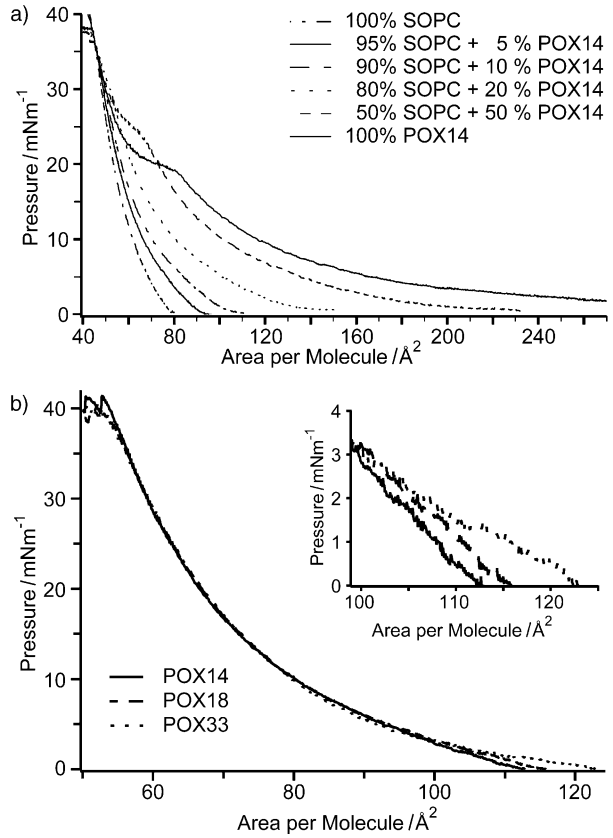

Figure 3. *a) Langmuir isotherms of various lipid/lipopolymer (POX14) mixtures recorded at 20 °C. Molar fractions of the lipopolymer ranged between 0 and 100 mol%, indicating that polymer–polymer interaction is negligible when the lipopolymer fraction is ≤20 mol%. b) Langmuir isotherms of SOPC monolayers with 5 mol% lipopolymer (POX14, POX18, and POX33), recorded at 20 °C. Little deviation among different polymer lengths could be seen at low surface pressures, presented in the inset.*

To investigate the influence of the polymer chain length on the lateral cooperativity within the monolayer, Langmuir isotherms of SOPC monolayers with 5 mol% lipopolymers were measured for POX18 and POX33 (Figure 3b). At this low molar fraction of lipopolymer, the stretching of polymer chains only appeared near the onset of the increase in surface pressure (inset, Figure 3b). When the film was compressed to higher surface pressures, the isotherms overlapped with each other up to $\pi = 40$ mN m^{-1}. The obtained results indicated that polymer–polymer interaction is also negligible for POX18 and POX33, if the molar fraction of the lipopolymer was kept at 5 mol%.

Since no phase separation could be observed from isotherms nor by fluorescence microscopy, one could assume a random distribution of the lipopolymers in the polymer/lipid monolayer. Therefore, the average distance between the lipopolymers can be approximated from the average molecular area measured at $\pi = 30$ mNm^{-1} ($A \sim 55$ Å^2), and from the molar fraction of lipopolymers ($f = 0.05 - 0.20$), $d = \sqrt{A/f}$. Since the radius of gyration, R_g, scales with $N^{1/2}$, we could approximate R_g from previous light scattering study of Chen et al.,[60] yielding $R_g \approx$ 1.7 nm for POX14, 1.9 nm for POX18, and 2.5 nm for POX33, respectively. Although the mean distance $d \approx 1.7$ nm at a lipopolymer fraction of 20 mol% matches with $R_g \approx 1.7$ nm for POX14, no polymer–polymer interaction was observed in the isotherms at this molar ratio (Figure 3a), since these values are rough approximations. Furthermore, as suggested from the isotherms (Figure 3b), interactions between the longer polymer chains (POX18 and POX33) are also negligible at a lipopolymer fraction of 5 mol% because the expected distance between polymer chains ($d \approx 3.3$ nm) is larger than R_g. This also excludes a polycondensation via the trimethoxysilane end groups of the lipopolymers prior to the deposition.[66]

Langmuir–Blodgett Deposition of Lipid/Lipopolymer Monolayers

After the compression, the monolayer was transferred from the air–water interface onto a solid substrate at a constant velocity. The transfer ratio, that is, ratio between the decrease in the subphase area and the area of the substrate, was found to be 1:1 for all samples. However, when the monolayer was transferred at a low transfer velocity (e.g., 50 μm s^{-1}), stripe-like patterns could be observed (see Figure 4a). These stripes were always aligned parallel to the transfer direction, as indicated by the arrow in the figure. It should be noted that such patterns are not formed due to a phase separation under thermodynamic equilibrium, because the fluorescence image of the same monolayer at air–water interface appeared homogeneous before the transfer. Furthermore, fluorescence labeling of lipopolymers confirmed that such stripe-like heterogeneities are formed by demixing of lipids and lipopolymers, but not by the segregation of fluorescence lipids (Purrucker et al. unpublished data). These findings strongly suggested that hydrodynamic conditions in the vicinity of the wetting front play a dominant role. When the transfer velocity was increased, these microscopic stripes became finer and finer and disappeared at a very high velocity (≥ 400 μm s^{-1}). As shown in Figure 5b, the fluorescence image of the monolayer with 5 mol% of POX14 was homogeneous over the entire substrate, but the transfer ratio still remained as 1:1. Fluorescence images of the monolayers transferred at this condition were found to be homogeneous at various lipopolymer fractions between 0 and 50 mol%.

Furthermore, the homogeneous distribution of lipopolymers within the monolayer was verified by experiments using analogous

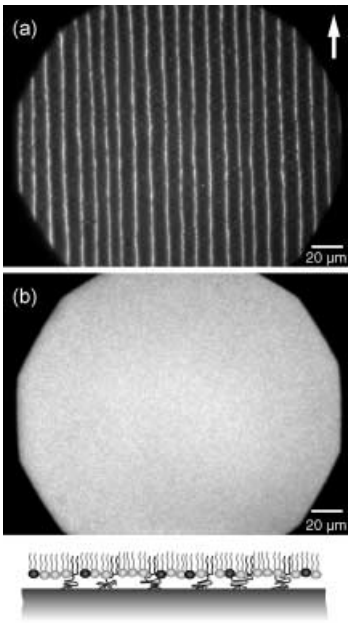

Figure 4. Fluorescence images of SOPC monolayers with 5 mol% POX14. The monolayers were transferred at velocities of a) 50 μm s^{-1} and b) 400 μm s^{-1}. The arrow denotes the direction of film transfer. Schematic illustration of the film is given at the bottom, representing fluorescence probes in black.

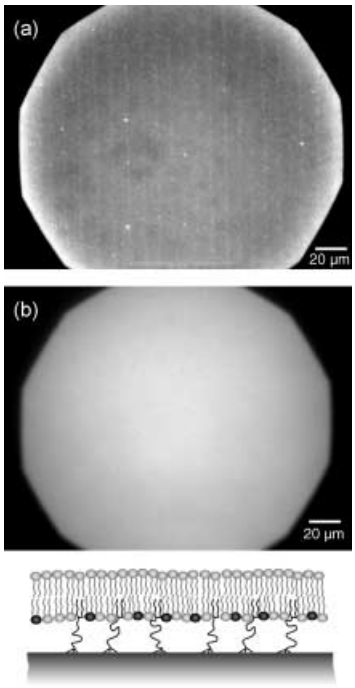

Figure 5. Fluorescence image of polymer-tethered membranes with 5 mol% POX14. The underlayer was labeled with 0.2 ol% of Texas Red-PE, and unlabeled SOPC vesicles were spread on the dry monolayers. Transfer velocities: a) 50 μm s^{-1}, b) 400 μm s^{-1}.

lipid/lipopolymer mixtures with fluorescence labeled lipopolymers (data not shown). Although the morphology of these stripe-like domains differs slightly, an increase in the transfer velocity led to a "thinning" of the stripe patterns. Indeed, for all the lipid/lipopolymer mixtures, we could prepare homogeneous monolayers without any loss of materials.

Heterogeneous "stripes" and "holes" either due to phase separation or to local defects have been reported in some of the previous studies. For example, Wagner and Tamm observed holes and stripe-like defects in the first lipid/lipopolymer layer with poly(ethylenoxide) lipopolymers, which could only be healed to some extent by spreading of the top layer.[28] Naumann et al.[36] used poly(2-ethyl-2-oxazoline) lipopolymers that were randomly grafted onto the surface by cross-linking to benzophenone groups. They also found macroscopic defects and phase separations at a lipopolymer concentration of 20 mol%. In contrast to these approaches, we demonstrated that systematic control of the hydrodynamic conditions during the transfer (i.e., transfer velocity) enables one to deposit homogeneous lipid/lipopolymer monolayers for various spacer lengths and concentrations.

Spreading of Top Layers by Vesicle Fusion

To verify the "self-healing" of heterogeneities in the underlayer as reported by Wagner and Tamm, we spread unlabeled SOPC vesicles on the labeled monolayer with stripe-like heterogeneities (Figure 5a). For the direct comparison, the monolayer was prepared under the same conditions as that presented in Figure 4a. As apparent from the figure, the spreading of the top layer as well as the swelling of polymer spacers seemed to induce the diffusion and mixing of lipids and lipopolymers, but a distinct heterogeneity in the underlayer still remains. Since the lipopolymers are most likely covalently attached to the surface and enriched in one of the domains, it is understandable that lateral diffusion of lipids cannot perfectly heal the "imprinted" heterogeneity. On the other hand, homogeneity of the monolayer prepared under the same conditions as that in Figure 4b was not disturbed by spreading of unlabeled SOPC vesicles (Figure 5b).

As the next step, labeled SOPC vesicles were spread onto the unlabeled underlayers. When the labeled vesicles were fused on a heterogeneous surface as described before, stripe-like domains could clearly be observed (Figure 6a). This strongly denotes that underlying heterogeneities in the underlayer disturb the homogeneous spreading of the top layer. To explain such a significant impact of the underlayer, there are two possible scenarios: 1) demixing of lipids and lipopolymers causes the mismatch in the lateral density of alkyl chains in lipid-enriched and lipopolymer-enriched domains that might even cause local defects, or 2) lateral diffusion of the lipids is disturbed by the high local concentration of grafted lipopolymer tethers. However, when the labeled vesicles were spread on a uniformly mixed lipid/lipopolymer monolayer, the top layer could coat the entire surface homogeneously (Figure 6b).

Diffusion Measurements

Since the fluidity of the lipid membrane strongly influences the function of membrane proteins, lateral diffusion constants of lipids in top and underlayers were measured by fluorescence

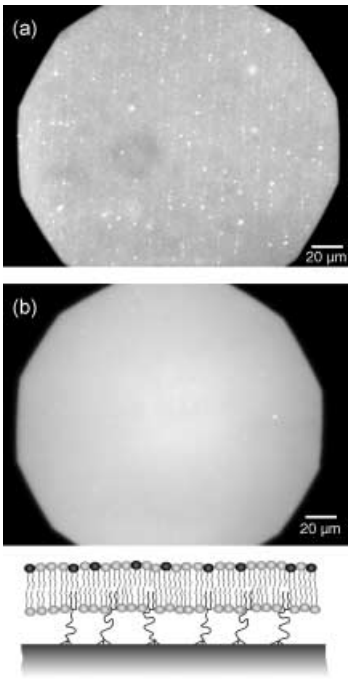

Figure 6. *Fluorescence image of polymer-tethered membranes with 5 mol% POX14. The underlayer was unlabeled, and SOPC vesicles labeled with 0.2 mol% of Texas Red-PE were spread on the dry monolayers. Transfer velocities: a) 50 μm s^{-1}, b) 400 μm s^{-1}.*

recovery after photobleaching (FRAP). Since the half time of the flip-flop exchange in fluid lipid bilayers are about 7 h to 10 days,[61, 62] the exchange of the lipids between inside and outside of the membrane is almost neglegible in our experimental time scale. As a control system, we deposited a pure SOPC membrane directly onto the bare substrate. The obtained diffusion constant ($D = 1.4\ \mu m^2 s^{-1}$) is in reasonable agreement with previously reported results.[28, 63] As summarized in Table 2 (upper panel), the increase in the molar fraction of lipopolymers (POX14) does not seem to influence the diffusion constants ($D = 0.9 - 1.6\ \mu m^2 s^{-1}$) or the mobile fractions (> 85%) within the lipopolymer fraction between 0 and 20 mol%. This range coincides well to that suggested from the Langmuir isotherms (Figure 3a), where the polymer – polymer interactions are negligible. In fact, when the lipopolymer fraction was increased to 50 mol%, the diffusion constant and mobile fraction decreased to $D = 0.4\ \mu m^2 s^{-1}$ and 10%, respectively. This can be attributed either to the increase in viscosity within interacting polymer chains in the water reservoir, or to the increase in the fraction of grafted lipopolymer tethers acting as obstacles.

Table 2. *Diffusion constants of lipids in the underlayers. Diffusion constants of lipids with various fractions of POX 14 (upper panel). Influence of the spacer length was studied for the membranes with 5 mol% of POX18 and POX33 (lower panel). The given diffusion constants are based on five individual measurements of different samples.*

Lipopolymer fraction	Lipopolymer	Diffusion constant D [$\mu m^2 s^{-1}$]	Mobile fraction [%]
0 mol%	-	1.4 ± 0.2	98 ± 3
5 mol%	POX14	1.6 ± 0.3	98 ± 4
10 mol%	POX14	0.9 ± 0.4	86 ± 12
20 mol%	POX14	1.3 ± 0.4	96 ± 2
50 mol%	POX14	0.4 ± 0.3	10 ± 1
5 mol%	POX18	1.4 ± 0.1	98 ± 2
5 mol%	POX33	1.4 ± 0.1	97 ± 3

As the next step, the impact of the spacer length was studied by measuring the diffusion constants of the membranes with 5 mol% of POX18 and POX33 (Table 2, lower panel). By choosing the same transfer speed (400 μm s^{-1}), homogeneous monolayers and bilayers could be deposited. Here, the increase in the spacer length caused no distinct decrease in the diffusion constants or in mobile fractions, suggesting that the higher sterical demands of the intermediate polymer chains did not increase the viscosity of the water reservoir. This agrees reasonably well with the Langmuir isotherms, where the spacer length showed almost no influence in the global shape of the isotherms of lipid/lipopolymer monolayers (Figure 3b).

The diffusion constants of lipids in the top layers were found to be almost constant within the experimental errors, $D = 1 - 2\ \mu m^2 s^{-1}$, independent from the underlying monolayers (data not shown). Since the alkyl chains incorporated in the underlayer were in all cases fluid and homogeneous, it is plausible that the friction between top- and underlayers is almost identical.[64]

From long term studies with repeated measurements of the diffusion constants of the polymer-tethered membranes, we found that all supported membranes were thermodynamically and mechanically stable for more than two weeks, showing no decrease in the membrane quality (homogeneity and fluidity) within the experimental error.

Tamm and co-workers[28] calculated the diffusion constant of the underlayer with longer ($n = 77$) poly(ethylenoxide) spacers from the bleached patterns (pattern width $\approx 10\ \mu m$). The diffusion constant was found to be $D = 0.4 - 1.8\ \mu m^2 s^{-1}$ for lipopolymer fractions of < 5 mol%, whereas it decreased to $D = 0.1 - 0.3\ \mu m^2 s^{-1}$ for the membranes with 5 – 10 mol% of lipopolymers. The mobile fractions they reported seem to be slightly smaller (80 ~ 90%) than those we found in this study. The difference in diffusion constants and mobile fractions of the underlayer can be related to an increase in the viscosity within the water reservoir. Naumann et al. bleached a quite large area (diameter: 150 μm) using a conventional fluorescence microscopy setup. For the underlayer with 5 mol% of lipopolymer ($n = 85$), they found the mobile fraction of 80% that agrees well with those reported by Tamm et al. However, the diffusion constant they measured ($D = 17.4\ \mu m^2 s^{-1}$, at 40 °C) seems to be unreasonably large. Such a large discrepancy might be due to a very slow bleaching rate (bleaching time: 10 s) as well as to the very large bleached area (diameter: 150 μm), which are 50 times longer and 15 times larger than our experimental systems, respectively.

Incorporation of Integrin $\alpha_{IIb}\beta_3$ into Polymer-Tethered Membranes

In order to test the feasibility and potential of the polymer-tethered membrane construct, we performed first experiments to incorporate transmembrane proteins within the bilayer. We

spread proteoliposomes with integrin $\alpha_{IIb}\beta_3$ onto the underlayers with 5 mol% of POX14, POX18, and POX33. For evaluation of the layer quality, the integrins were labeled with 5(6)-TAMRA-SE prior to the preparation of proteoliposomes. Again, as a control experiment, proteoliposomes were firstly spread on a glass substrate, resulting in fragmented domains of proteins (Figure 7a). Prolonged incubation time could not increase the homogeneity of the protein distribution, indicating that the local defects cannot be healed by the fusion of single patches.[8] When proteoliposomes were incubated with the underlayer with 5 mol% POX14, one could clearly see fluorescent "circles" on the surface, whose diameter is approximately 10 μm (Figure 7b). At present, we could not conclude whether these "circles" correspond to the fused proteoliposomes adherent to the surface or to the clusters of integrins. Spreading of proteoliposomes onto underlayers with 5 mol% of POX18 or POX33, resulting in a very different picture (Figure 7c and 7d). A homogeneous distribution of integrins on the surface can clearly be seen. Although one could still see small clusters that might correspond to locally aggregating integrins, the entire surface is uniformly coated with polymer-tethered membranes containing integrins. The macroscopically homogeneous distribution of integrins in the membranes with longer polymer spacers (POX18 and POX33) suggests that the substrate–membrane distance is one of the key parameters for successful incorporation of transmembrane receptors.[65] Our preliminary FRAP experiments on the membrane with 5 mol% of POX33 revealed the lateral diffusion constant of integrins and the mobile fraction of 0.03 $\mu m^2 s^{-1}$ and 20%, respectively. Not only to determine the substrate–membrane spacing but also to quantify the orientation and distribution of the integrins in the bilayer, more systematic FRAP experiments are being carried out at different lipopolymer fractions and protein concentrations. Nevertheless, the results obtained here strongly suggest the potential of the tethered membranes with well-defined length and distribution of soft polymer spacers for stress-free incorporation of sterically demanding transmembrane receptors with large extracellular domains.

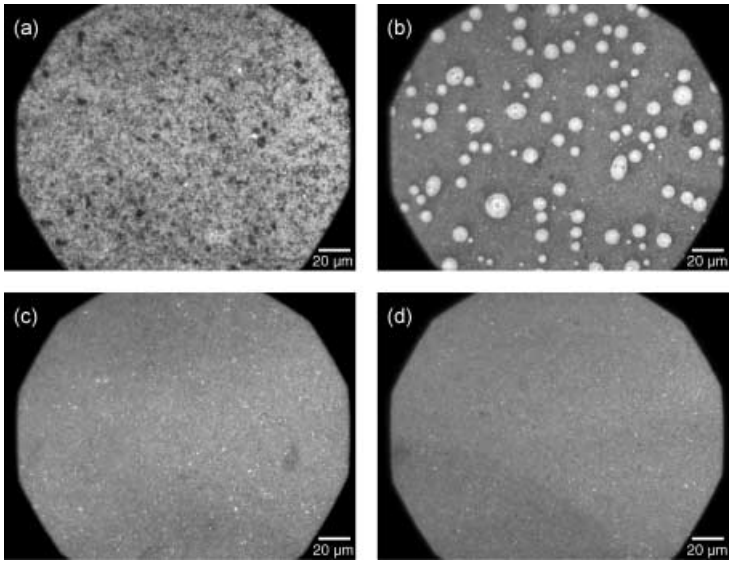

Figure 7. *Fluorescence images of proteoliposomes with fluorescent labeled integrin $\alpha_{IIb}\beta_3$ spread on a) bare glass slide, b) monolayer with 5 mol% of POX14, c) monolayer with 5 mol% of POX18, and d) monolayer with 5 mol% of POX33.*

Conclusions

In this study, we fabricated polymer-tethered lipid membranes using tailored poly(2-oxazoline) lipopolymers. The supported membranes were prepared by LB transfer of lipid/lipopolymer mixtures, followed by fusion of small lipid vesicles. Careful optimization of each step of the preparation resulted in homogeneous and stable membranes. The influence of the spacer length and density upon the lateral diffusion of lipids could quantitatively be determined by FRAP. Furthermore, preliminary results showed that the spacer length strongly influences the homogeneity of integrin $\alpha_{IIb}\beta_3$ receptors on the surface, suggesting a large potential of this strategy towards immobilization of various transmembrane proteins on solid surfaces.

Acknowledgements

This work was financially supported by the Deutsche Forschungsgemeinschaft (SFB 563, Project B7) and the Fonds der Chemischen Industrie. The authors are grateful to E. Sackmann, H. Ringsdorf, and C. Erdelen for fruitful discussions. O.P. and M.T. are thankful to M. Rusp for purification of integrins. M.T. is thankful to the DFG for the Emmy Noether fellowship.

Keywords: cell receptors · fluorescence recovery after photobleaching (FRAP) · lipopolymers · membranes

[1] L. K. Tamm, H. M. McConnell, *Biophys. J.* **1985**, *47*, 105.
[2] E. Sackmann, *Science* **1996**, *271*, 43.
[3] J. T. Groves, S. G. Boxer, *Acc. Chem. Res.* **2002**, *35*, 149.
[4] P. Y. Chan, M. B. Lawrence, M. L. Dustin, L. M. Ferguson, D. E. Golan, T. A. Springer, *J. Cell Biol.* **1991**, *115*, 245.
[5] M. L. Dustin, L. M. Ferguson, P. Y. Chan, T. A. Springer, D. E. Golan, *J. Cell Biol.* **1996**, *132*, 465.
[6] E.-M. Erb, K. Tangemann, B. Bohrmann, B. Müller, J. Engel, *Biochemistry* **1997**, *36*, 7395.
[7] S. Y. Qi, J. T. Groves, A. K. Chakraborty, *Proc. Natl. Acad. Sci. USA* **2001**, *98*, 6548.
[8] S. Gönnenwein, M. Tanaka, B. Hu, L. Moroder, E. Sackmann, *Biophys. J.* **2003**, *48*, 646.
[9] S. J. Johnson, T. M. Bayerl, D. C. McDermott, G. W. Adam, A. R. Rennie, R. K. Thomas, E. Sackmann, *Biophys. J.* **1991**, *59*, 289.
[10] B. W. Koenig, S. Krueger, W. J. Orts, C. F. Majkrzak, N. F. Berk, J. V. Silverton, K. Gawrisch, *Langmuir* **1996**, *12*, 1343.
[11] P. Fromherz, V. Kiessling, K. Kottig, G. Zeck, *Appl. Phys. A* **1999**, *69*, 571.
[12] V. Kiessling, L. K. Tamm, *Biophys. J.* **2003**, *84*, 408.
[13] E. Sackmann, M. Tanaka, *Trends Biotechnol.* **2000**, *18*, 58.
[14] W. Knoll, C. W. Frank, C. Heibel, R. Naumann, A. Offenhäuser, J. Rühe, E. K. Schmidt, W. W. Shen, A. Sinner, *Rev. Mol. Biotechnol.* **2000**, *74*, 137.
[15] H. Hillebrandt, G. Wiegand, M. Tanaka, E. Sackmann, *Langmuir* **1999**, *15*, 8451.
[16] S. Gritsch, P. Nollert, F. Jähning, E. Sackmann, *Langmuir* **1998**, *14*, 3118.

[17] M. Tanaka, S. Kaufmann, J. Nissen, M. Hochrein, *Phys. Chem. Chem. Phys.* **2001**, *3*, 4091.
[18] R. Häussling, W. Knoll, H. Ringsdorf, F.-J. Schmitt, J. Yang, *Makromol. Chem. Macromol. Symp.* **1991**, *46*, 145.
[19] C. Heibel, S. Maus, W. Knoll, J. Rühe, in *Organic Thin Films—Structure and Applications, Vol. 695* (Ed.: C. W. Frank), American Chemical Society, **1998**, p. 104.
[20] J. Spinke, J. Yang, H. Wolf, M. Liley, H. Ringsdorf, W. Knoll, *Biophys. J.* **1992**, *63*, 1667.
[21] C. Erdelen, L. Häussling, R. Naumann, H. Ringsdorf, H. Wolf, J. Yang, *Langmuir* **1994**, *10*, 1246.
[22] M. Seitz, E. Ter-Ovanesyan, M. Hausch, C. K. Park, J. A. Zasadzinski, R. Zentel, J. N. Israelachvili, *Langmuir* **2000**, *16*, 6067.
[23] P. Théato, R. Zentel, *Langmuir* **2000**, *16*, 1801.
[24] H. Lang, C. Duschl, H. Vogel, *Langmuir* **1994**, *10*, 197.
[25] B. A. Cornell, V. Braach-Maksvytis, L. G. King, P. D. J. Osman, B. Raguse, L. Wieczorek, R. J. Pace, *Nature* **1997**, *387*, 580.
[26] B. Raguse, V. Braach-Maksvytis, B. A. Cornell, L. G. King, P. D. J. Osman, R. J. Pace, L. Wieczorek, *Langmuir* **1998**, *14*, 648.
[27] S. M. Schiller, R. Naumann, K. Lovejoy, H. Kunz, W. Knoll, *Angew. Chem.* **2003**, *115*, 219; *Angew. Chem. Int. Ed.* **2003**, *42*, 208.
[28] M. L. Wagner, L. K. Tamm, *Biophys. J.* **2000**, *79*, 1400.
[29] M. L. Wagner, L. K. Tamm, *Biophys. J.* **2001**, *81*, 266.
[30] N. Bunjes, E. K Schmidt, A. Jonczyk, F. Rippmann, D. Beyer, H. Ringsdorf, P. Gräber, W. Knoll, R. Naumann, *Langmuir* **1997**, *13*, 6188.
[31] E. K. Schmidt, T. Liebermann, M. Kreiter, A. Jonczyk, R. Naumann, A. Offenhäuser, E. Neumann, A. Kukol, A. Maelicke, W. Knoll, *Biosens. Bioelectron.* **1998**, *13*, 585.
[32] R. Jordan, K. Graf, H. Riegler, K. K. Unger, *Chem. Commun.* **1996**, 1025.
[33] R. Jordan, K. Martin, H. J. Räder, K. K. Unger, *Macromolecules* **2001**, *34*, 8858.
[34] A. Förtig, R. Jordan, O. Purrucker, M. Tanaka, *Polymer Preprints* **2003**, *44*, 850.
[35] W. W. Shen, B. S. G. Boxer, W. Knoll, C. W. Frank, *Biomacromolecules* **2001**, *2*, 70.
[36] C. A. Naumann, O. Prucker, T. Lehmann, J. Rühe, W. Knoll, C. W. Frank, *Biomacromolecules* **2002**, *3*, 27.
[37] F. Brochard-Wyart, P. G. de Gennes, *Adv. Colloid Interface Sci.* **1992**, *39*, 1.
[38] G. Elender, E. Sackmann, *J. Phys. II* **1994**, *4*, 455.
[39] F. Rehfeldt, M. Tanaka, L. Pagnoni, R. Jordan, *Langmuir* **2002**, *18*, 4908.
[40] W. Kern, D. A. Puotinen, *RCA Rev.* **1970**, *31*, 187.
[41] P. Persigehl, R. Jordan, O. Nuyken, *Macromolecules* **2000**, *33*, 6977.
[42] E. Kalb, S. Frey, L. K. Tamm, *Biochim. Biophys. Acta* **1992**, *1103*, 307.
[43] A. L. Plant, *Langmuir* **1993**, *9*, 2764.
[44] O. Purrucker, H. Hillebrandt, K. Adlkofer, M. Tanaka, *Electrochim. Acta* **2001**, *47*, 791.
[45] M. Keller, J. Schilling, E. Sackmann, *Rev. Sci. Instrum.* **2001**, *72*, 3626.
[46] D. Axelrod, D. E. Koppel, J. Schlessinger, E. Elson, W. W. Webb, *Biophys. J.* **1976**, *16*, 1055.
[47] D. M. Soumpasis, *Biophys. J.* **1983**, *41*, 95.
[48] B. Müller, H.-G. Zerwes, K. Tangemann, J. Peter, J. Engel, *J. Biol. Chem.* **1993**, *268*, 6800.
[49] B. Hu, D. Finsinger, K. Peter, Z. Guttenberg, M. Bärmann, H. Kessler, A. Escherich, L. Moroder, J. Böhm, W. Baumeister, S. Sui, E. Sackmann, *Biochemistry* **2000**, *39*, 12284.
[50] L. Fitzgerald, B. Leung, D. Phillips, *Anal. Biochem.* **1985**, *151*, 169.
[51] C. R. Woese, G. E. Fox, *Proc. Natl. Acad. Sci. USA* **1977**, *74*, 5088.
[52] J. C. Mathai, G. D. Sprott, M. L. Zeidel, *J. Biol. Chem.* **2001**, *276*, 27266.
[53] W. H. Velander, R. D. Madurawe, A. Subramanian, G. Kumar, G. Sinai-Zingde, J. S. Riffle, *Biotechnol. Bioeng.* **1992**, *39*, 1024.
[54] M. C. Woodle, C. M. Engbers, S. Zalipsky, *Bioconjugate Chem.* **1994**, *5*, 493.
[55] T. Lehmann, J. Rühe, *Macromol. Symp.* **1999**, *142*, 1.
[56] D. D. Lasic, D. Needham, *Chem. Rev.* **1995**, *95*, 2601.
[57] T. R. Baekmark, T. Wiesenthal, P. Kuhn, T. M. Bayerl, O. Nuyken, R. Merkel, *Langmuir* **1997**, *13*, 5521.
[58] T. R. Baekmark, I. Sprenger, M. Ruile, O. Nuyken, R. Merkel, *Langmuir* **1998**, *14*, 4222.
[59] M. B. Foreman, J. P. Coffmann, M. J. Murcia, S. Cesana, R. Jordan, G. S. Smith, C. A. Naumann, *Langmuir* **2003**, *19*, 326.
[60] F. P. Chen, A. E. Ames, L. D. Taylor, *Macromolecules* **1990**, *23*, 4688.
[61] R. D. Kornberg, H. M. McConnell, *Biochemistry* **1971**, *10*, 1119.
[62] J. E. Rothmann, E. A. Dawidowicz, **1975**.
[63] R. Merkel, E. Sackmann, E. Evans, *J. Phys. Chem. Solids* **1989**, *50*, 1535.
[64] E. Evans, E. Sackmann, *J. Fluid Mech.* **1988**, *194*, 553.
[65] To measure membrane-substrate distance more quantitatively, we additionally carried out fluorescence interference contrast microscopy experiments (courtesy of P. Fromherz's lab). The obtained membrane-substrate distances for POX14 and POX18 are about 2 nm, which is quite close to the limit of the technique. On the other hand, the corresponding value for POX33 was about 5 nm (Purrucker et al., unpublished data).[66]
[66] Remark added in the proof. Very recent and more reliable fluorescent correlation spectroscopy measurements of poly(2-methyl-2-oxazoline)s in water gave a hydrodynamic radius for the $n = 26$ polymer of $R_h = 1.0 \pm 0.2$ nm. This radius would result in an R_h for POX14 = 0.7 nm, POX18 = 0.8 nm, and POX33 = 1.1 nm. This result agrees much better with our LB results (T. Bonné, K. Lüdtke, R. Jordan, P. Stepanek, C. M. Papadakis, unpublished results).

Received: June 5, 2003 [F 863]

